Incorporation of Titanium into Mesoporous Silica Molecular Sieve SBA-15

Zhaohua Luan, Estelle M. Maes, Paul A. W. van der Heide, Dongyuan Zhao, Roman S. Czernuszewicz, and Larry Kevan*

Department of Chemistry, University of Houston, Houston, Texas 77204-5641

Received August 9, 1999

Mesoporous silica molecular sieve SBA-15 has been synthesized and incorporated with variable amounts of titanium via incipient-wetness impregnation with titanium isopropoxide in ethanol followed by calcination. Characterization by powder X-ray diffraction, nitrogen adsorption, X-ray photoelectron, Raman, and diffuse reflectance ultraviolet spectroscopies has been carried out to understand the chemical nature of the titanium. The results suggest that titanium is present in two distinct chemical forms and that their relative amounts depend on the titanium loading. At low titanium loading of 1 atom % relative to silicon, the titanium ions are monatomically dispersed and the pore size of SBA-15 is not altered. This isolated titanium species reaches a maximum concentration around 6 atom % relative to silicon. At higher titanium loading, titanium dioxide (anatase) is also formed. The materials with significant titanium dioxide formation have reduced pore diameters, which suggests that the titanium dioxide exists as a thin film anchored inside the mesopores of SBA-15. This new material may have potential as a novel catalyst.

Introduction

Titanium dioxide supported on amorphous silica has been studied as a catalyst and as a catalytic support.[1−6] It has been found that the microstructural nature and dispersion of the titanium dioxide is rather dependent on the preparation procedures. More recently, titanium dioxide has been grafted onto mesoporous MCM-41 and FSM-16 silica materials, and it was concluded that nanosized TiO_2 clusters were formed inside the pores but that anatase TiO_2 only formed as a minor phase on the external surface.[7] TiO_2/silica systems are also of current interest as photocatalysts.[8−10]

As a counterpoint to supported titanium dioxide, isolated titanium ions have also been incorporated into microporous and mesoporous crystalline silica materials. The best known is perhaps TS-1, which is silicalite-1 with part of the silicons substituted by titanium.[11,12] TS-1 is an effective catalyst for selective oxidation of a variety of organic compounds in dilute hydrogen peroxide. Titanium has also been substituted into the framework of various materials,[13] including microporous aluminophosphates[14,15] and mesoporous silica MCM-41.[16−18] Incorporation of titanium into these materials is generally achieved via a "direct synthesis" procedure which involves addition of a titanium source, such as titanium isopropoxide in ethanol, to the gel for hydrothermal synthesis.

SBA-15 is a newly discovered mesoporous silica molecular sieve with uniform tubular channels variable from 50 to 300 Å.[19,20] Incorporation of either framework titanium or titanium nanoparticles into SBA-15 by direct synthesis appears unlikely because SBA-15 is synthesized in strong acidic media (2 M HCl). However, titanium incorporation might be achieved by "post-synthesis" grafting procedures involving reaction with a titanium ion solution.[7,21] This procedure has been used

(1) Reichmann, M. G.; Bell, A. T. *Appl. Catal.* **1987**, *32*, 315.
(2) Fernandez, A.; Leyrer, J.; González-Elipe, A. R.; Munuera, G.; Knözinger, H. *J. Catal.* **1988**, *112*, 489.
(3) Munoz-Paet, A.; Munera, G. In *Preparation of Catalysts V*; Poncelet, G., Jacobs, P. A., Grange, P., Delmon, B., Eds.; Studies in Surface Science and Catalysis, Vol. 63; Elsevier: Amsterdam, 1991; p 627.
(4) Srinivasan, S.; Datye, A. K.; Hampden-Smith, M.; Wachs, I. E.; Deo, G.; Jehng, J. M.; Turek, A. M.; Peden, C. H. F. *J. Catal.* **1991**, *131*, 260.
(5) Castillo, R.; Koch, B.; Ruiz, P.; Delmon, B. *J. Mater. Chem.* **1994**, *4*, 903.
(6) Castillo, R.; Koch, B.; Ruiz, P.; Delmon, B. *J. Catal.* **1996**, *161*, 524.
(7) Aronson, B. J.; Blanford, C. F.; Stein, A. *Chem. Mater.* **1997**, *9*, 2842.
(8) Fernández, A.; Lassaletta, G.; Jimenez, V. M.; Justo, A.; González-Elipe, A. R.; Hermann, J.-M.; Tahiri, H.; Ait-lchou, Y. *Appl. Catal. B* **1995**, *7*, 49.
(9) Xu, Y.; Langford, C. H. *J. Phys. Chem. B* **1997**, *101*, 3115.
(10) Ahn, S. W.; Kevan, L. *J. Chem. Soc., Faraday Trans.* **1998**, *94*, 3147.
(11) Notari, B. *Adv. Catal.* **1996**, *41*, 253.
(12) Prakash, A. M.; Kevan, L. *J. Catal.* **1998**, *178*, 586.
(13) Bellussi, G. and Rigutto, M. S. In *Advanced Zeolite Science and Applications*; Jansen, J. C., Stöcker, M., Karge, H. G., Weitkamp, J., Eds.; Studies in Surface Science and Catalysis, Vol. 85; Elsevier: Amsterdam, 1994; pp 177−213.
(14) Prakash, A. M.; Kurshev, V.; Kevan, L. *J. Phys. Chem. B* **1997**, *101*, 9794.
(15) Prakash, A. M.; Kevan, L.; Zahedi-Niaki, M. H.; Kaliaguine, S. *J. Phys. Chem. B*, **1999**, *103*, 831.
(16) Corma, A.; Navarro, M. T.; Pariente, J. P. *J. Chem. Soc., Chem. Commun.* **1994**, 147.
(17) Alba, M. D.; Luan, Z.; Klinowski, J. *J. Phys. Chem.* **1996**, *100*, 2178.
(18) Prakash, A. M.; Sung-Suh, H. M.; Kevan, L. *J. Phys. Chem. B* **1998**, *102*, 857.
(19) Zhao, D.; Feng, J.; Huo, Q.; Melosh, N.; Fredrickson, G. H.; Chmelka, B. F.; Stucky, G. D. *Science* **1998**, *279*, 548.
(20) Zhao, D.; Huo, Q.; Feng, J.; Chmelka, B. F.; Stucky, G. D. *J. Am. Chem. Soc.* **1998**, *120*, 6024.

10.1021/cm9905141 CCC: $18.00
Published on Web 11/25/1999

successfully to attach titanium as titanocene or titanium isopropoxide onto the walls of mesoporous MCM-41.[21,22] It has been suggested that the titanium complex is anchored to silanol groups and forms highly dispersed titanium sites after calcination. Such materials show higher activity for liquid-phase oxidation in contrast to materials made by direct synthesis. This has been attributed to more accessible titanium sites or to a decrease in the silanol concentration.[22,23]

In this work, we report postsynthesis procedures to incorporate titanium into SBA-15 as a framework species and to prepare thin TiO_2 molecular films anchored inside the mesopores of SBA-15. X-ray diffraction (XRD), nitrogen adsorption, diffuse reflectance ultraviolet, X-ray photoelectron (XPS), and Raman spectroscopies have been used to characterize these two forms of titanium in SBA-15.

Experimental Section

Samples. A synthesis for mesoporous silica SBA-15 has been reported.[19,20] In our typical synthesis, 2 g of amphiphilic triblock copolymer, poly(ethylene glycol)-*block*-poly(propylene glycol)-*block*-poly(ethylene glycol) (average molecular weight 5800, Aldrich), was dispersed in 15 g of water and 60 g of 2 M HCl with stirring, followed by addition of 4.25 g of tetraethyl orthosilicate (Aldrich) to the homogeneous solution with stirring. This gel was stirred at 40 °C for 24 h and then crystallized in a Teflon-lined autoclave at 100 °C for 2 days. After crystallization, the solid product was centrifuged, filtered, washed with deionized water, and dried in air at room temperature. The material was calcined in static air at 550 °C for 24 h to decompose the triblock copolymer and obtain a white powder (SBA-15).

Titanium-incorporated SBA-15, designated as TiSBA-15, was prepared in a shallow dish inside a glovebox under flowing nitrogen. Titanium was loaded into SBA-15 at room temperature by incipient-wetness impregnation.[24] For every 1 g of SBA-15, varying amounts of titanium isopropoxide in 10 g ethanol were used. The titanium concentration in the solution varies from 0.05 to 5.00 M, depending on the desired titanium loading. The impregnated material was dried under flowing nitrogen at room temperature for 2 days. Calcination was performed in static air at 550 °C for 5 h. These samples are designated as TiSBA-15-(*x*), where *x* is the stoichiometric Si/Ti molar ratio from the incipient-wetness impregnation. For convenience, we will refer to these nominal Si/Ti ratios throughout even though the analyzed ratios of the synthesized samples are lower. For comparison, TiO_2 (anatase) powder was used as received from Aldrich.

Characterization. Powder XRD patterns were collected before and after calcination using a Scintag PADX diffractometer equipped with a liquid nitrogen-cooled germanium solid-state detector using Cu Kα radiation. The samples were prepared as thin layers on aluminum slides.

Nitrogen adsorption isotherms were measured at 77 K using a Micromeritics Gemini 2375 analyzer. The volume of adsorbed N_2 was normalized to standard temperature and pressure. Prior to the experiments, samples were dehydrated at 250 °C for 5 h. The specific surface area, A_{BET}, was determined from the linear part of the BET equation ($P/P_0 = 0.05-0.31$). The calculation of the pore size distribution was performed using the desorption branches of the N_2 adsorption isotherms and the Barrett−Joyner−Halenda (BJH) formula.[25] Although the BJH analysis underestimates the pore size,[26−29] relative changes in the pore size should be accurately portrayed. The mesopore surface area, A_{BJH}, and mesopore volume, V_{BJH}, were obtained from the pore size distribution curves. The average mesopore diameter, D_{BJH}, was calculated as $4V_{BJH}/A_{BJH}$.

Diffuse reflectance electronic spectra were measured with a Perkin-Elmer 330 spectrophotometer equipped with a 60 mm Hitachi integrating sphere accessory. Powder samples were loaded in a quartz cell with Suprasil windows, and spectra were collected in the wavelength range from 200 to 1000 nm against a siliceous SBA-15 standard.

X-ray photoelectron spectra were collected on a Physical Electronics model 5700 instrument using monochromatic Al Kα X-rays at 1486 eV operated at 350 W. The analyzer (Omni focus V electrostatic lens and hemispherical mirror analyzer) was operated in the fixed retard ratio mode at a pass energy of 11.75 eV. Charge neutralization, necessary for the analysis of these samples, was accomplished via a newly developed dual-beam technique that employs a combination of a low-energy electron beam and a low-energy (~5 eV) Ar^+ ion beam directed toward the analyzed region.[30] The former compensates for the removal of secondary, photo-, and Auger electrons, and the latter alleviates static charge buildup occurring in and around the analyzed region. The area analyzed and the collection solid cone were fixed to 1100 mm and 5°, respectively. A resolution of 0.51 eV fwhm is attainable under these conditions. The Shirley background-subtraction routine[31] was used throughout, and the O(1s), Si(2p), and Ti(2p) binding energies were referenced to the C(1s) line situated at 285.0 eV.

Raman spectra were obtained at room temperature using a 514.5 nm line from a Coherent 90-6 Ar^+ ion laser by collecting backscattered photons directly off the stationary surface of a 1 cm diameter and about 0.05 cm thick disk of the sample. Details of this sampling technique have been presented elsewhere.[32] A conventional scanning Raman instrument equipped with a Spex 1403 double monochromator (with 1800 grooves/mm gratings) and a Hamamatsu 928 photomultiplier detector was used to record all spectra under the control of a Spex DM3000 microcomputer system. The laser power was set to 150 mW except for the samples showing very strong scattering properties (TiSBA-15-(5), TiSBA-15-(1), and TiO_2), for which a much lower laser power (20 mW) was used. All spectra were recorded from 200 to 1300 cm^{-1} with spectral slit widths of 5 cm^{-1} (3 cm^{-1} for TiSBA-15-(5), TiSBA-15-(1), and TiO_2). The spectrometer was advanced in 1 cm^{-1} increments. Integration time was 1 s per data point for all spectra. In the case of SBA-15 and TiSBA-15-(*x*), where $x = 10$, 20, 40, 80, multiple scans (eight) were averaged to improve the signal-to-noise ratio. The slowly sloping baselines were subtracted from the digitally collected spectra by using LabCalc software (Galactic Industries) mounted on a 486-DX 66 MHz PC microcomputer.

Results

Sample Analysis. Low-angle XRD patterns of siliceous SBA-15 and TiSBA-15 are similar. A well-resolved pattern with a prominent peak at 0.8° and two weak

(21) Hagen, A.; Wei, D.; Haller, G. L. In *Mesoporous Molecular Sieves*; Bonneviot, L., Beland, F., Danumah, C., Kaliaguine, S., Eds.; Studies in Surface Science and Catalysis, Vol. 117; Elsevier: Amsterdam, 1998; pp 191−200.
(22) Maschmeyer, T.; Rey, F.; Sankar, G.; Thomas, J. M. *Nature* **1995**, *378*, 159.
(23) Tatsumi, T.; Koyano, K. A.; Igarashi, N. *Chem. Commun.* **1998**, 325.
(24) Gao, X.; Bare, S. R.; Fierro, J. L. G.; Banares, M. A.; Wachs, I. E. *J. Phys. Chem. B* **1998**, *102*, 5653.
(25) Barrett, E. P.; Joyner, L. G.; Halenda, P. P. *J. Am. Chem. Soc.* **1951**, *73*, 373.
(26) Ravikovitch, P. I.; Wei, D.; Chueh, W. T.; Haller, G. L.; Neimark, A. V. *J. Phys. Chem. B* **1997**, *101*, 3671.
(27) Kruk, M. Jaroniec, M.; Sayari, A. In *Proceedings of the 12th International Zeolite Conference*; Treacy, M. J., Marcus, B. K., Bisher, M. E., Higgins, J., Eds.; Materials Research Society: Warrendale, PA, 1999; pp 761−766.
(28) Lukens, W. W., Jr.; Schmidt-Winkel, P.; Zhao, D.; Feng, J.; Stucky, G. D. *Langmuir* **1999**, *15*, 5403.
(29) Kruk, M.; Jaroniec, M. *Langmuir* **1999**, *15*, 5279.
(30) Moulder, J.; Hook, D. *Phi Interface* **1997**, *17*, 1.
(31) Briggs, D.; Shea, M. P. *Practical Surface Analysis*, 2nd ed.; Wiley: New York, 1990.
(32) Czernuszewicz, R. S. *Appl. Spectrosc.* **1986**, *40*, 571.

Table 1. XPS Si/Ti Ratios and O(1s) and Ti(2p) Binding Energies[a] of Mesoporous TiSBA-15 Molecular Sieves

materials	(Si/Ti)xps	O(1s) (eV)		Ti($2p_{3/2}$) (eV)	Ti($2p_{3/2}$)/(eV)[b] LBE		HBE	
SBA-15		533.1						
TiSBA-15-(80)	36	533.1		459.7	458.8	(16.7)	459.8	(83.3)
TiSBA-15-(40)	24	533.1	530.2	459.5	459.0	(32.9)	459.9	(67.1)
TiSBA-15-(20)	8.4	533.1	530.3	459.2	459.2	(68.6)	460.0	(31.4)
TiSBA-15-(10)	5.0	533.1	530.2	459.5	459.3	(70.4)	460.3	(29.6)
TiSBA-15-(5)	3.9	533.0	530.3	459.0	458.9	(74.9)	459.9	(25.1)
TiSBA-15-(1)	0.6	533.0	530.2	458.9	458.9	(92.1)	459.9	(7.9)
TiO_2 (anatase)			530.1	458.8				

[a] Referenced to the C(1s) peak at 285.0 eV. [b] LBE and HBE refer to the low and high binding energy contributions observed in the curve fitting of the respective spectra. The relative contributions in percentage are given in parentheses.

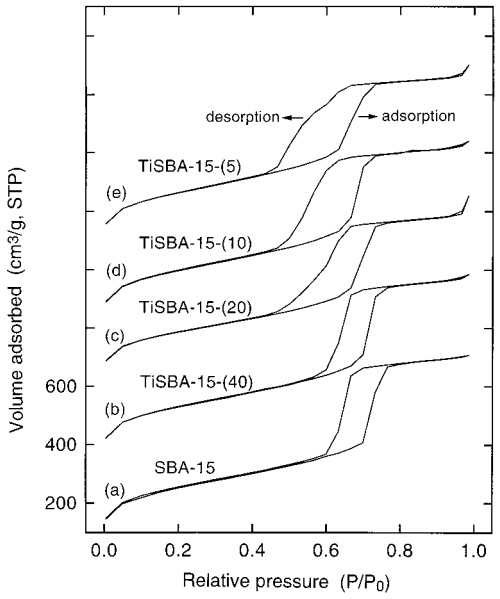

Figure 1. Adsorption−desorption isotherms of nitrogen at 77 K of TiSBA-15 materials with varying titanium loading corresponding to Si/Ti molar ratios of (a) ∞, (b) 40, (c) 20, (d) 10, and (e) 5. The vertical scale is given for isotherm a; the other isotherms are displaced upward to avoid overlap.

peaks at 1.6 and 1.7° 2θ are observed that match well with the pattern reported for SBA-15.[19] The XRD peaks can be indexed to a hexagonal lattice with a $d(100)$ spacing of 99.1 Å, corresponding to a large unit cell parameter $a_0 = 114$ Å ($a_0 = 2d(100)/(3)^{1/2}$). Calcination does not affect the XRD patterns except for increasing the signal intensity. The Si/Ti ratios of the synthesized samples were analyzed by XPS and are about half of the ratios based on the chemical stoichiometry from the incipient wetness impregnation (Table 1).

Nitrogen Adsorption. *N_2 Adsorption Isotherms.* Figure 1 shows N_2 adsorption isotherms from calcined siliceous SBA-15 and TiSBA-15 with varying titanium loading. All materials give typical irreversible type IV adsorption isotherms with a H1 hysteresis loop as defined by IUPAC.[33] N_2 adsorption at low relative pressure ($P/P_0 < 0.31$) is accounted for by monolayer adsorption of N_2 on the pore walls and does not indicate the presence of micropores. The calculated BET or total specific surface area of SBA-15 is around 1000 m^2/g and seems to decrease with increasing titanium loading (Table 2). However, the mesopore surface areas (A_{BJH})

Table 2. Pore Structure Parameters of TiSBA-15 Calculated from the Desorption Branch of Nitrogen Adsorption Isotherms Using the Barrett−Joyner−Halenda Formula

materials	A_{BET} (m^2/g)	A_{BJH} (m^2/g)	V_{BJH} (cm^3/g)	D_{BJH} (Å)
SBA-15	997	926	1.17	50.5
TiSBA-15-(80)	835	789	1.02	51.5
TiSBA-15-(40)	764	692	0.88	51.0
TiSBA-15-(20)	742	758	0.89	47.2
TiSBA-15-(10)	691	737	0.81	44.3
TiSBA-15-(5)	804	870	0.92	42.4

do not indicate a decreasing trend with titanium loading. As the relative pressure increases ($P/P_0 > 0.31$), the isotherms from siliceous SBA-15, TiSBA-15-(80) (not shown) and TiSBA-15-(40) with low titanium loading exhibit sharp inflections in the P/P_0 range from 0.60 to 0.80, characteristic of capillary condensation within uniform pores (Figure 1a,b). The P/P_0 position of the inflection points is clearly related to a diameter in the mesopore range, and the sharpness of these steps indicates the uniformity of the mesopore size distribution. With additional titanium loading, the TiSBA-15 materials give isotherms with similar inflection but with reduced sharpness and a shift toward lower P/P_0 values over a larger P/P_0 range (Figure 1c−2c).

Pore Size Distribution. The BJH pore size distribution is based on the Kelvin equation and has been widely used for mesoporous materials.[34] However, recent work suggests that the Kelvin equation should be modified to obtain more accurate pore sizes.[26−29] Because we are principally interested in **changes** in the pore size distribution, we can use the BJH values for this purpose. Average BJH values of the pore diameter D_{BJH} are given in Table 2 and show a significant decrease compared to those of SBA-15 for Si/Ti = 20 and less. The structure of the pore size distribution is more clearly shown in Figure 2. SBA-15 shows a very narrow pore size distribution with an average diameter of 55 Å. This average diameter is also found for TiSBA-15-(80) (not shown) and TiSBA-15-(40), but the half-width for the distribution increases by about 20% for Si/Ti = 40. At Si/Ti = 20 a bimodal pore distribution is observed, and the smaller pore of about 40 Å dominates more as the titanium content further increases.

Diffuse Reflectance Ultraviolet−Visible Spectroscopy. Figure 3 shows ultraviolet spectra of a series of TiSBA-15 materials. At low titanium loading corresponding to Si/Ti = 80, the observed absorption band maximum is at 230 nm (Figure 3a). For increasing

(33) Sing, K. S. W.; Everett, D. H.; Haul, R. A. W.; Moscow, L.; Pierotti, R. A.; Rouquerol, J.; Siemieniewska, T. *Pure Appl. Chem.* **1985**, *57*, 603.

(34) Tanev, P. T.; Vlaev. L. T. *J. Colloid Interface Sci.* **1993**, *160*, 110.

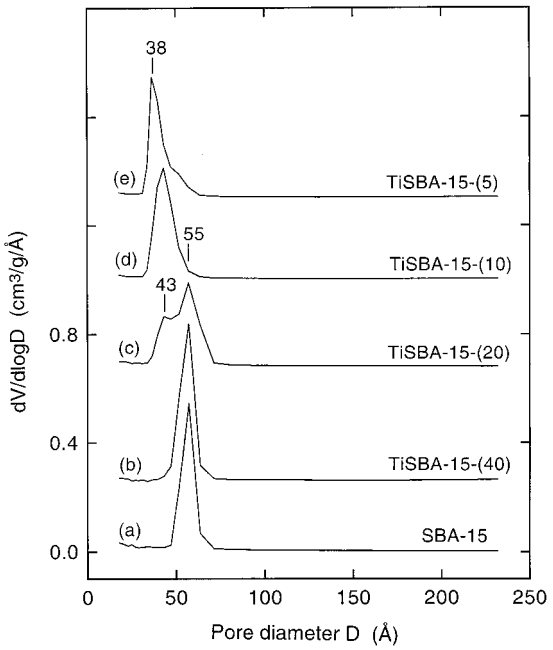

Figure 2. Pore size distribution curves for TiSBA-15 materials with varying titanium loading corresponding to Si/Ti molar ratios of (a) ∞, (b) 40, (c) 20, (d) 10, and (e) 5. The vertical scale is given for distribution a; the other distributions are displaced upward to avoid overlap.

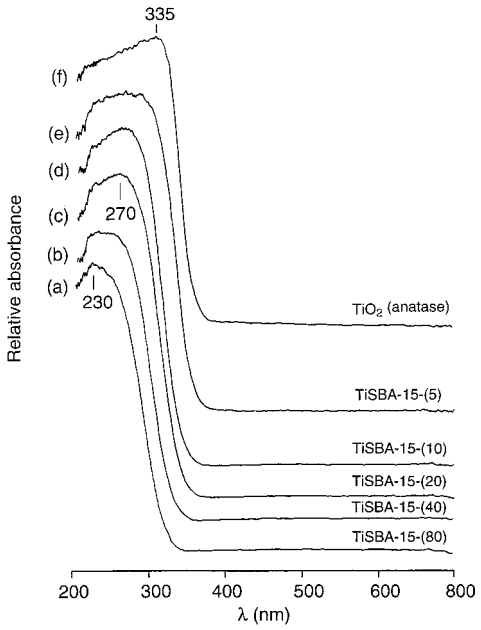

Figure 3. Diffuse reflectance UV−visible spectra of TiSBA-15 materials with varying titanium loading corresponding to Si/Ti molar ratios of (a) 80, (b) 40, (c) 20, (d) 10, (e) 5, and (f) TiO_2 anatase. The baselines are displaced vertically to avoid overlap.

titanium loading, the maximum shifts to near 270 nm (Figure 3c), and its intensity increases somewhat with increasing titanium content. The 230 nm band still seems present (Figure 3b−d). Further increase in titanium loading to Si/Ti = 5 shows a broad absorption band over the 230−340 nm range (Figure 3e), which is blueshifted from the spectrum of bulk TiO_2 anatase (Figure 3f).

X-ray Photoelectron Spectroscopy. Figure 4 shows O(1s) XPS spectra of TiSBA-15 with varying titanium

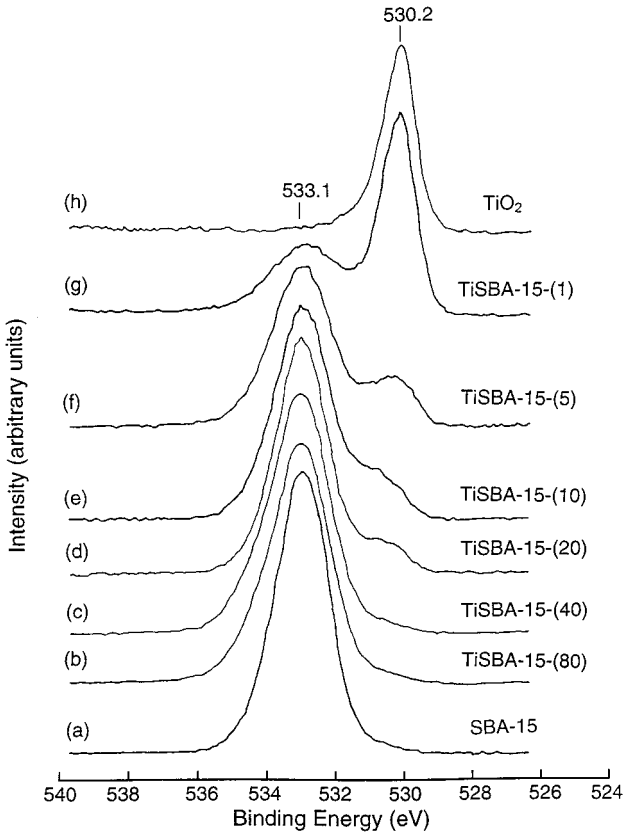

Figure 4. O(1s) XPS spectra of TiSBA-15 materials with varying titanium loading corresponding to Si/Ti molar ratios of (a) ∞, (b) 80, (c) 40, (d) 20, (e) 10, (f) 5, (g) 1, and (h) TiO_2 anatase. The baselines are displaced vertically to avoid overlap.

loading. Only an intense O(1s) line at 533.1 eV is observed for siliceous SBA-15 and TiSBA-15 with low titanium loading corresponding to Si/Ti > 40 (Figure 4a−c). With increasing titanium loading, a weak O(1s) line at 530.2 eV becomes resolvable, and its intensity increases relative to the O(1s) line at 533.1 eV (Figure 4d−g). TiO_2 anatase gives only one O(1s) line at 530.2 eV (Figure 4 h).

Figure 5 shows Ti(2p) XPS spectra as a Ti($2p_{3/2}$) and Ti($2p_{1/2}$) doublet with a separation of 5.75 eV[35] for TiSBA-15 with varying titanium loading. With low titanium loading, TiSBA-15-(80) shows a Ti($2p_{3/2}$) line at 459.7 eV binding energy, which is about 1 eV higher than that of TiO_2 anatase (Figure 5a,f). With increasing titanium loading the positions of the Ti(2p) lines shift toward lower binding energies and become narrower (Figure 5b,c). In addition, some asymmetry on the high-binding-energy (HBE) side of the titanium doublet is noted at low titanium loading. As the titanium loading further increases for Si/Ti < 5, the Ti($2p_{3/2}$) line shifts further to 458.8 eV (Figure 5d,e), which is closer to the binding energy of Ti($2p_{3/2}$) measured for TiO_2 anatase (Figure 5f).

For a series of TiSBA-15 materials with varying titanium loading, the Ti(2p) doublet can be reasonably well fitted with two symmetric curves for a low-binding-energy (LBE) component and an HBE component as

(35) *Handbook of X-ray Photoelectron Spectroscopy*; Chastain, J., King, R. C., Jr., Eds.; Physical Electronics, Inc.: Minneapolis, Minnesota, 1995.

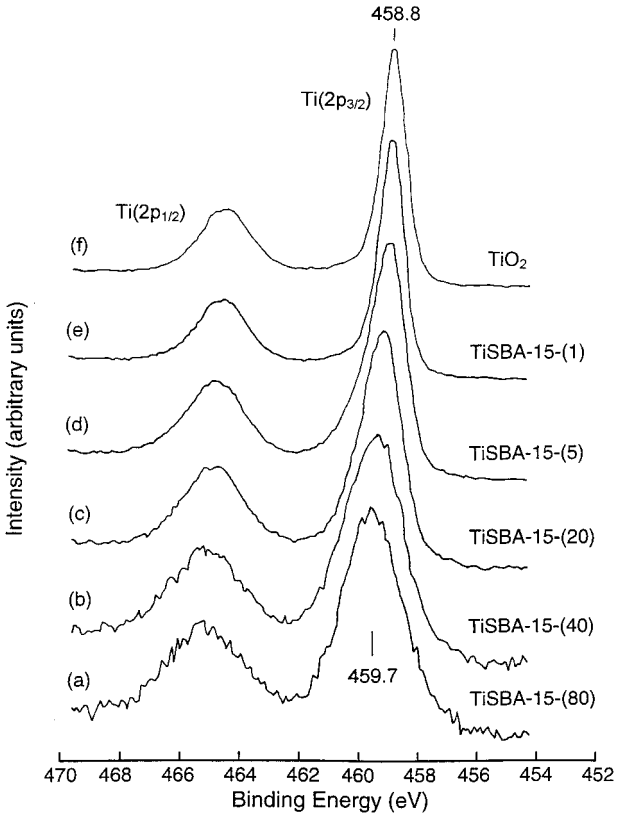

Figure 5. Ti(2p) XPS spectra of TiSBA-15 materials with varying titanium loading corresponding to Si/Ti molar ratios of (a) 80, (b) 40, (c) 20, (d) 5 and (e) 1, and (f) TiO_2 anatase. The baselines are displaced vertically to avoid overlap.

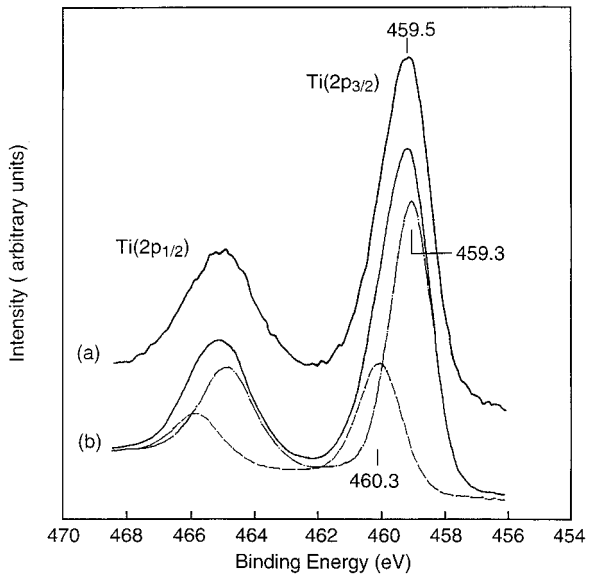

Figure 6. (a) Ti(2p) XPS spectrum from a TiSBA-15 sample with a Si/Ti molar ratio of 10 and (b) spectral decomposition into two components shown by dashed lines and their sum shown by a solid line. The baselines are displaced vertically to avoid overlap.

shown in Figure 6 for TiSBA-15-(10). In all cases, the area of the Ti($2p_{1/2}$) peak was fixed at 50% of the area of the Ti($2p_{3/2}$) peak and their separation was fixed at 5.75 eV.[35] Additional support for the use of two components is shown by the fact that all spectra could be fitted by adjusting the relative contributions of the two

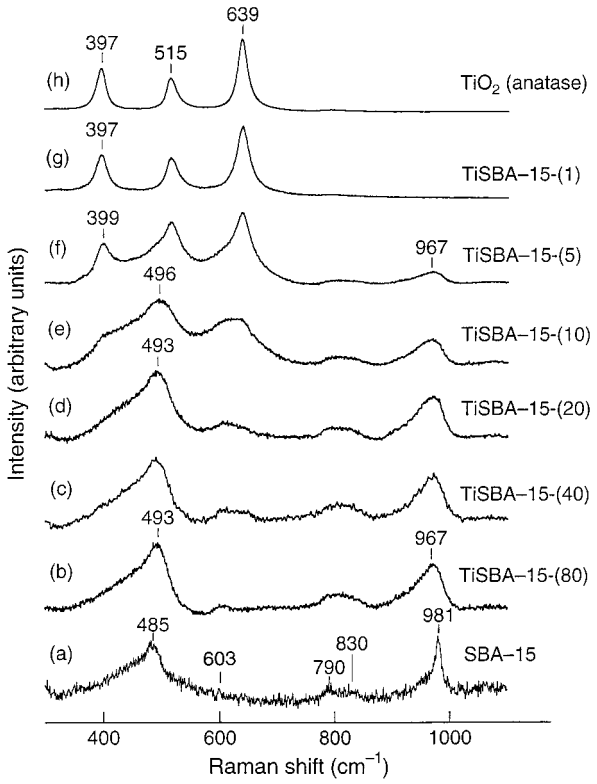

Figure 7. Raman spectra of TiSBA-15 materials with varying titanium loading corresponding to Si/Ti molar ratios of (a) ∞, (b) 80, (c) 40, (d) 20, (e) 10, (f) 5, (g) 1, and (h) TiO_2 anatase. The baselines are displaced vertically to avoid overlap.

doublets. All binding energy values and relative areas for the two contributions are listed in Table 1.

Raman Spectroscopy. Figure 7 shows the Raman spectra of a series of TiSBA-15 samples with variable titanium content. Siliceous SBA-15 exhibits spectroscopic features similar to those of amorphous SiO_2[36,37] except that the line at 981 cm^{-1} is more intense in SBA-15 (Figure 7a). On the basis of previous literature assignments for silicate materials,[36,37] the bands at 790 and 830 cm^{-1} are assigned to siloxane linkages (Si−O−Si), and the bands at 485 and 603 cm^{-1} to four- and three-membered siloxane rings, respectively. The 981 cm^{-1} band in siliceous SBA-15 can be assigned to a surface silanol (O_3Si−OH) stretching vibration, which is consistent with a previous assignment for a weak band in the 980−990 cm^{-1} region for amorphous SiO_2 (Cab-O-Sil).[37,38] With titanium present, the sharp band at 981 cm^{-1} due to surface silanol groups is not observable even at low titanium loading (Figure 7b), while another broad band at 967 cm^{-1} develops. As the titanium loading increases, a significant spectral change occurs (Figure 7b−g). At Si/Ti = 10, the observed Raman spectrum (Figure 7e) resembles one previously reported for fumed silica coated with titanium dioxide.[4] Very intense Raman bands at 397, 515, and 639 cm^{-1} can be detected for samples with high titanium loading (Figure 7f−h), which are characteristic of TiO_2 anatase.[39]

(36) Went, G. T.; Oyama, S. T.; Bell, A. T. *J. Phys. Chem.* **1990**, *94*, 4240.
(37) Das, N.; Eckert, H.; Hu, H.; Wachs, I. E.; Walzer, J. F.; Feher, F. J. *J. Phys. Chem.* **1993**, *97*, 8240.
(38) de Man, A. J. M.; Sauer, J. *J. Phys. Chem.* **1996**, *100*, 5025.
(39) Deo, G.; Turek, A. M.; Wachs, I. E.; Huybrechts, D. R. C.; Jacobs, P. A. *Zeolites* **1993**, *13*, 365.

Discussion

Mechanism for Low Titanium Loading. Siliceous SBA-15 gives a Raman band at 981 cm^{-1} assigned to silanol groups on the wall surfaces (Figure 7a). In comparison with MCM-41 materials,[40] this band is weaker for SBA-15. This may be due to the much thicker walls of SBA-15[20] compared to those of MCM-41 so that the concentration of silanol groups is lower. Incorporation of titanium reduces the intensity of the 981 cm^{-1} band, which suggests that the silanol groups on SBA-15 serve as active sites for titanium grafting and are consumed. This was previously suggested for silica materials with titanium dioxide coatings.[4]

A band near 960 cm^{-1} has been previously observed in spectra of various titanium-substituted silicalites and has been recently reassigned from silanol[13,41] or titanyl (Ti = O)[42] stretching modes to an asymmetric Ti−O−Si stretching mode on the basis of quantum mechanical calculations.[38] We tentatively assign the 967 cm^{-1} Raman band for TiSBA-15 similarly so that it seems associated with incorporated titanium. However, with increasing titanium loading, the intensity of the 967 cm^{-1} Raman band is constant for Si/Ti of 80−20, but it does decrease for lower Si/Ti ratios. This decrease is attributed to the formation of titanium dioxide particles or films (see below). Then, the constant intensity for Si/Ti = 80−20 is consistent with increasing formation of TiO_2 as the titanium loading increases.

Chemical Nature of Titanium versus Loading. For TiSBA-15 materials with variable Si/Ti ratios, specific information about the chemical nature of the incorporated titanium can be derived from ultraviolet, Raman, and XPS results.

Ultraviolet spectra. Absorption spectroscopy has been extensively used to characterize the nature and coordination of titanium ions in titanium-substituted molecular sieves and supported TiO_2 nanoparticle materials.[11,13,43,44] The ultraviolet absorption wavelength of titanium is sensitive to its coordination and to TiO_2 particle size, especially for sizes less than 10 nm.[45] For TiSBA-15-(80) with low titanium loading (Si/Ti = 80), the absorption maximum at 230 nm has been observed for various zeolite materials that contain tetrahedral titanium like TS-1 and has been assigned to a charge-transfer transition between the oxygen ligands and a central Ti^{4+} ion with tetrahedral coordination.[11,13] This suggests that the titanium is highly dispersed in TiSBA-15 with low titanium loading. For Si/Ti = 5, the broad absorption band near 290 nm is blueshifted from the 335 nm band for bulk TiO_2 anatase. Such a blueshift has been observed for dispersed TiO_2 nanoparticles on silica[7,24] and is so interpreted here. Thus, at high titanium loading in TiSBA-15, the ultraviolet spectra are consistent with TiO_2 particle formation.

Raman Spectra. Raman spectroscopy is extremely sensitive to TiO_2 nanoparticles with a minimum detectable amount of 0.05 wt % in TiO_2−SiO_2 mixed oxides due to its strong scattering properties.[24] No characteristic bands due to TiO_2 anatase are observed for TiSBA-15 when the titanium loading is low, but intense Raman bands occur for high titanium loading, which is characteristic of TiO_2 anatase particles.[39] The Raman results suggest that isolated titanium ions are present in TiSBA-15 at low titanium loading but that TiO_2 anatase-like domains are present when the loading is relatively high.

XPS Spectra. Only an intense O(1s) line at 533.1 eV is observed for siliceous SBA-15 and for TiSBA-15 with low titanium loading corresponding to Si/Ti > 40 (Figure 4a−c). This line can be assigned to oxygen in an SiO_2 environment in TiSBA-15.[45] Because TiO_2 gives a O(1s) line at 530.2 eV (Figure 4 h),[46] the absence of a second O(1s) line at this binding energy indicates that titanium incorporation with these loadings does not much alter the original electronic environment for oxygen in SBA-15 and is consistent with little if any TiO_2 in TiSBA-15 with Si/Ti > 40. This supports the suggestion that titanium is monatomically dispersed in these samples. However, with increasing titanium loading, a second O(1s) line appears (Figure 4d−g), which can be attributed to oxygen in a TiO_2 environment.[36]

The information derived from O(1s) XPS spectra of TiSBA-15 is echoed in the corresponding Ti(2p) XPS spectra of the same materials. The Ti(2p) lines of TiSBA-15 with low titanium content contain an unusual doublet with binding energies significantly higher than those for titanium in TiO_2 (Figure 5a−c), indicating that the titanium is present in a different environment from that in TiO_2. The shift with respect to titanium in TiO_2 is about 1 eV toward higher energy. This could be associated with a difference in titanium coordination. On the basis of previous assignments for TiO_2−SiO_2 glasses[47,48] and for titanosilicate molecular sieve TS-1[41,46] where titanium is known to be in tetrahedral coordination, this shift to higher energy is attributed to tetrahedrally coordinated titanium in TiSBA-15. This suggests a monatomic dispersion of Ti(IV) ions in TiSBA-15 with low titanium loading. The increase in Ti(2p) binding energy can be explained by an increase of the interatomic potentials due to a decrease of the coordination number of titanium and a shortening of the Ti−O bond. The silicalite lattice may maintain high electron densities on the oxygen atoms that surround a tetrahedral titanium atom to make the titanium more electropositive and the Ti−O bond more ionic. Because it has been shown that titanium silicalites such as TS-1, which are active for epoxidation of olefins, have a high Ti(2p) binding energy,[13,41] TiSBA-15 may also serve as an effective catalyst for some selective oxidation reactions.

With increasing titanium loading, the position of the Ti(2p) lines shifts toward 458.9 eV, close to the energy measured for TiO_2 anatase (Figure 5d−f). The Ti(2p)

(40) Luan, Z.; Meloni, P. A.; Czernuszewicz, R. S.; Kevan, L. *J. Phy. Chem. B* **1997**, *101*, 9046.
(41) Scarano, D.; Zecchina, A.; Bordiga, S.; Geobaldo, F.; Spoto, G.; Petrini, G.; Leofanti, G.; Padovan, M.; Tozzola, G. *J. Chem. Soc., Faraday Trans.* **1993**, *89*, 4123.
(42) Notari, B. In *Innovation in Zeolite Materials Science*; Grobet, P. J., Mortier, W. J., Vansant, E. F., Schulz-Ekloff, G., Eds.; Studies in Surface Science and Catalysis, Vol. 37; Elsevier: Amsterdam, 1988; pp 413−425.
(43) Tuel, A. *Zeolites* **1995**, *15*, 228.
(44) Luan, Z.; Kevan, L. *J. Phys. Chem. B* **1997**, *101*, 2020.
(45) Davis, R. J.; Liu, Z. *Chem. Mater.* **1997**, *9*, 2311.
(46) Grohmann, I.; Pilz, W.; Walther, G.; Kosslick, H.; Tuan, V. A. *Surf. Interface Anal.* **1994**, *22*, 403.
(47) Mukhopadhyay, S. M.; Garofalini, S. H. *J. Non-Cryst. Solids* **1990**, *126*, 202.
(48) Stakheev, A. Y.; Shpiro, E. S.; Apijok, J. *J. Phys. Chem.* **1993**, *97*, 5668.

Table 3. Calculated Titanium Coordination from XPS Data for TiSBA-15 Molecular Sieves

material	$Ti(tet)/(Ti(tet) + Ti(oct))_{xps}$	$(Ti(tet)/(Si + Ti(tet))_{xps}$
TiSBA-15-(80)	0.83	0.023
TiSBA-15-(40)	0.67	0.027
TiSBA-15-(20)	0.31	0.036
TiSBA-15-(10)	0.30	0.056
TiSBA-15-(5)	0.25	0.061

line with a $Ti(2p_{3/2})$ binding energy of 458.9 eV can be assigned to Ti(IV) with octahedral coordination. This suggests that a titanium dioxide film develops with increasing titanium loading.

The curve fitting profiles of an HBE component [speculated to be titanium in tetrahedral coordination, Ti(tet)] and an LBE component [speculated to be titanium in octahedral coordination, Ti(oct)] (Table 3) reveal that, at low titanium loading, up to 83% of the titanium is present as the HBE species and that this percentage declines with increasing titanium incorporation. The absolute percentages from this analysis are considered to be less accurate than the trend. We do not consider that 17% of the Ti is present as TiO_2 at low loading because Raman spectroscopy, which is particularly sensitive to TiO_2, indicates no TiO_2 at low loading. The last column in Table 3 shows an upper limit of about 6% of the silicons that can be substituted by titanium in SBA-15 silicas. A similar limit has been observed in amorphous TiO_2-SiO_2 glasses and various titanosilicate molecular sieves where titanium substitutes for framework silicons.[13]

Overall, ultraviolet absorption, XPS, and Raman spectroscopies suggest that at low titanium loading the anchored titanium is tetrahedrally coordinated and dispersed as isolated titanium ions. There is an upper limit of about 6% of the silicons that can be substituted by titanium in TiSBA-15. For increasing titanium loading, the spectroscopic results suggest the existence of a titanium dioxide film that is well-dispersed over the internal wall surfaces of TiSBA-15.

Titanium Dioxide Film Formation. The Raman, ultraviolet, and XPS data all indicate the formation of TiO_2 anatase at high titanium loading. Furthermore, the probable involvement of the silanol groups within the mesopores of SBA-15 in the mechanism of titanium grafting suggests that the TiO_2 phase is produced within the mesopores. Direct evidence for this location is shown by the pore size distribution in Figure 2. A logical interpretation of the bimodal pore size distribution for TiSBA-15-(20) is the formation of a titanium dioxide film on the walls of the 55 Å diameter mesopores. For reduction to 43 Å diameter as in Figure 2c,d, this implies a 6 Å thick film, which seems consistent with one to two monolayers of TiO_2. The bimodal pore size distribution largely disappears for TiSBA-15-(10); so, we might assume complete TiO_2 coverage of the mesopore walls at that titanium loading. Then, from the BET surface area of 839 m^2/g for siliceous SBA-15, which is the surface area before the TiO_2 film is formed, and the measured $Si/Ti = 5$ for TiSBA-15-(10), the number of titanium atoms per gram of SBA-15 divided by the surface area is 2.4 Ti/nm^2. This is less than the value of 5.5 Ti/nm^2 for the surface Ti density of an anatase 010 plane,[24] which may indicate that at $Si/Ti = 5$ in TiSBA-15 the TiO_2 film is not a complete monolayer.

Conclusions

Mesoporous silica molecular sieve SBA-15 has been synthesized and incorporated with titanium via incipient-wetness impregnation with titanium isopropoxide in ethanol followed by calcination. Adsorption and spectroscopic results reveal that the titanium is monatomically dispersed as titanium ions on SBA-15 silica wall surfaces at low titanium loading, whereas a titanium dioxide anatase film is formed at high titanium loading. The TiSBA-15 materials retain a large surface area, but the pore diameter decreases as the titanium dioxide film is formed. The abundant surface silanol groups are suggested to be involved in the titanium incorporation. These TiSBA-15 materials may be potentially useful as selective oxidation catalysts for large organic molecules or as photocatalysts for the degradation of organic contaminants.

Acknowledgment. This research was supported by the Robert A. Welch Foundation, the University of Houston Energy Laboratory, and the National Science Foundation. This includes the MRSEC program of the National Science Foundation under award Number DMR-9632667.

CM9905141